Biogeochemistry (2015) 122:131–150
DOI 10.1007/s10533-014-0035-6

Spatiotemporal variations in carbon dynamics during a low flow period in a carbonate karst watershed: Santa Fe River, Florida, USA

Jin Jin · Andrew R. Zimmerman · Jonathan B. Martin · Mitra B. Khadka

Received: 24 June 2014 / Accepted: 5 September 2014 / Published online: 12 September 2014

Abstract To understand role of biogeochemical reactions in controlling the amount and molecular form of dissolved carbon exported from carbonate terrains, spatiotemporal variations in dissolved organic carbon (DOC) and dissolved inorganic carbon (DIC) were observed over one year in the Santa Fe River system, a period of base flow or below. A water mixing model developed using concentrations of Na^+, Cl^-, and SO_4^{-2} identified three major water sources: soil water, groundwater and deep aquifer water. After accounting for mixing of these water sources, additional chemical signatures resulting from biogeochemical processes in the riparian zone were identified. Net mineralization of DOC occurred throughout the Santa Fe River watershed, particularly during the lowest flow conditions and in the upper watershed. However, natural dissolved organic matter was more labile during low flow and in the lower watershed, and predominantly derived from groundwater (rather than soil water) in all samples, likely via releases during carbonate dissolution. Carbonate dissolution commonly occurred in the upper watershed during low flow conditions, while carbonate minerals precipitated during baseflow, as well as in the lower watershed during very low flow conditions. Thus, riparian zone biogeochemical processes were strongly mediated by watershed hydrology, whose spatiotemporal variations resulted in greater inorganic and organic C export production in the lower watershed than the upper watershed, and during higher flow versus lower flow periods. During this lower flow period, the Santa Fe River watershed exported ~1.0 and 10.3 ton km^{-2} $year^{-1}$ DOC and DIC, respectively, representing higher C yields than many other types of watersheds.

Keywords Dissolved organic carbon · Dissolved inorganic carbon · Biogeochemical processes · Hydrologic mixing model · Carbon cycling · Karst

Responsible Editor: Jonathan Sanderman.

Electronic supplementary material The online version of this article (doi:10.1007/s10533-014-0035-6) contains supplementary material, which is available to authorized users.

J. Jin · A. R. Zimmerman (✉) · J. B. Martin · M. B. Khadka
Department of Geological Sciences, University of Florida, 241 Williamson Hall, P.O. Box 112120, Gainesville, FL 32611, USA
e-mail: azimmer@ufl.edu

Introduction

Karst is an important geomorphic feature that covers 20 % of the Earth's ice-free land surface and is composed of sinkholes, springs, and streams that sink into subsurface caverns (Ford and Williams 2007). Globally, carbonate rocks in karst terrains contain about 6.1×10^7 Pg of carbon (C), or about four orders of magnitude greater than the amount in the ocean,

which is the next largest reservoir (Falkowski et al. 2000; Houghton and Woodwell 1989). The annual atmospheric CO_2 sink from carbonate weathering has recently been estimated to be 0.5 Pg of C (Liu et al. 2011), which is about one tenth of the amount released annually by the combustion of fossil fuels globally (Quay 1992; Watson et al. 1990). Watersheds developed in carbonate terrains provide crucial processes affecting the global carbon cycle, as they have been reported to act both as a sink (Liu and Zhao 2000; Martin et al. 2013; Probst et al. 1994; Telmer and Veizer 1999) and source (Berner 1999; Berner and Lasaga 1989; Martin et al. 2013) of C. However, how C is produced/consumed/transformed/transported within karst watersheds remains unclear, largely due to the lack of knowledge on biogeochemical processes, water–rock interactions, and surface water-groundwater interactions within karst watersheds (Dreybrodt 1988; Ford and Williams 2007; White 1988).

Natural dissolved organic matter (NDOM) is derived mainly from microbes and plants and their degradation products and its chemical composition is complex and heterogeneous (Findlay and Sinsabaugh 2003; Frimmel 1998). It can be involved in a number of abiotic and biotic processes in karst watersheds and thus influences water quality. Abiotic processes may include carbonate mineral dissolution/precipitation and NDOM-mineral sorption/desorption (Davis 1982; Hoch et al. 2000; Inskeep and Bloom 1986; Jin and Zimmerman 2010; Jin et al. 2014; Lin and Singer 2005). Biotic transformations of NDOM in a karst watershed may include microbial consumption, production or other processes such as sorption/desorption onto/off mineral surface (Lovley and Chapelle 1995, 1996). NDOM also directly or indirectly control the quality of the natural waters. For instance, the presence of subsurface NDOM can influence the mobility of heavy metals (Lee et al. 2005; Petrovic et al. 1999) and thus, may be of concern to human health. As important as NDOM can be, few studies have addressed the transportation and transformation of NDOM in karst watersheds and how it influences environmental aspects like water quality and riverine ecology.

This study aims to improve the understanding of biogeochemical processes affecting reactions involving inorganic and organic C in karst watersheds. During periods of elevated rainfall, runoff, and river flow, large inputs of particulate and dissolved soil C, high CO_2 evasion rates, and carbonate dissolution affect variations in riverine C dynamics (Jin et al. 2014; Khadka et al. 2014). This study was conducted during a low flow year when biogeochemical processes would have a greater influence on C cycling and export than hydrologic effects. In addition, as recent climate change studies indicate that the southeastern United States is experiencing a long-term drying trend (Burke et al. 2006; CCSP 2008; IPCC 2007; Pearlstine 2009; Selman et al. 2013), studying riverine biogeochemistry during a low flow period may provide insights into projected future conditions.

There are three main objectives of this study: 1) identify possible endmember water sources, 2) assess the relative contributions of these sources, and 3) investigate the biogeochemical processes that control the spatial and temporal variations in the quantity and quality of organic and inorganic C. We used a multiple tracer approach to address these research questions. The tracers include dissolved organic carbon (DOC) and dissolved inorganic carbon (DIC) as well as dissolved ions, stable isotopes, spectrophotometric characteristics of NDOM, and other water chemistry parameters. We hypothesize that, as riverine NDOM undergoes microbial respiration, concentrations of DOC should decrease away from recharge areas, while DIC, as a product of mineralization, should increase in concentration (Alberic and Lepiller 1998; Aravena et al. 2004; Batiot et al. 2003; Lee and Krothe 2001; Lindroos et al. 2002; McCarthy et al. 1996; Pabich et al. 2001; Rauch and Drewes 2004). This simple relationship may be complicated by other reactions such as mineral dissolution/precipitation and sorption/desorption. Consequently, we examine other parameters such as pH, specific conductivity (SpC), and concentrations of Ca and Mg in our analyses.

Study area

The Santa Fe River watershed (Fig. 1) drains water into the Suwannee River from 3,585 km^2 of forests, agricultural land and small towns in north Florida. The watershed is entirely underlain by the upper Floridan aquifer (UFA), which is composed of Oligocene and Eocene carbonate rocks. The aquifer is confined by siliciclastic rocks of the Miocene Hawthorn Group in the eastern portion of the watershed and unconfined in

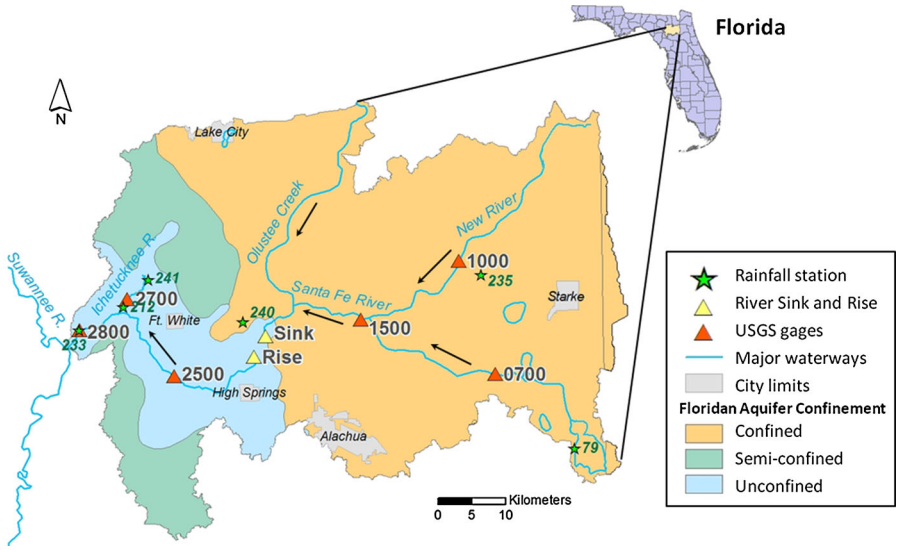

Fig. 1 The Santa Fe River watershed in north Florida showing hydrogeologic regimes, rainfall stations and sampling sites at six USGS gage stations and River Sink and River Rise in the O'Leno State Park. (Color figure online)

the western portion (Fig. 1). Precipitation is seasonal with approximately half of the average annual precipitation of 140 cm year^{-1} occurring in the summer between June and September. Recharge rates to the confined UFA were determined to be <30 cm year^{-1} while recharge to the unconfined portion is 40–80 cm year^{-1} (Grubbs 1998) although recharge is also seasonal because of elevated evapotranspiration during the summer (Martin and Gordon 2000).

The boundary between confined and semi-confined/unconfined portions of the UFA is marked by the Cody Scarp, a marine terrace that is the erosional edge of the Hawthorn Group (Scott 1988). Where the Santa Fe River crosses the Cody Scarp, it flows into the 'River Sink' and flows approximately 7 km underground, re-emerging at the at a first magnitude spring called the River Rise (Martin and Dean 2001). The Cody Scarp marks the boundary between the upper watershed that is dominated by wetlands and tree plantations and the lower watershed that is primarily improved pasture (see land use map provided in Supplemental materials Fig. S1). Distinct river water compositions with high levels of DOC, low SpC, comparatively high levels of P and low levels of N in the upper watershed and, low DOC, high SpC, high N and low P concentrations in the lower watershed have been reported (Katz 1992). Surface water-groundwater exchange is pervasive at the Cody Scarp (Martin and Dean 2001; Upchurch and Lawrence 1984), but its extent depends on flow. Following large rainfall events, flows are dominated by overland runoff, creating a blackwater (DOC-rich) phase along the entire course of the river. In contrast, during low rainfall periods groundwater discharges to the river through numerous springs and seeps in the lower watershed. Although these broad patterns of mixing between surface water and groundwater are known, less is known of how NDOM character varies at low flow when the DOC-rich water of the upper watershed mix extensively with the DIC rich waters of the lower watershed (Khadka et al. 2014).

Methods

Field sampling

During eight sampling trips between June 2010 and May 2011, surface water samples were collected at six USGS gauging stations and the River Sink and River Rise along the Santa Fe River and two of its major tributaries (Fig. 1). The gauging stations, from upstream to downstream, were #23220700, #23221000 (on the New River), #23221500, #23222500, #23222700 (on the Ichetucknee River), and #23222800. In the following paper, the Santa Fe watershed designation (#2322xxxx) is dropped and each site is referred to by the final three or four digits, e.g., 700, 1,000, 1,500, 2,500, 2,700, and 2,800. No sample was collected at 2,500 in June 2010 due to severe weather. New River was deemed to be the main trunk of the river for the purposes of this study

because of its greater length and higher flow compared to the upper reach of the Santa Fe River.

Surface water samples were collected from the shore using a peristaltic pump (Geotech Geopump 2) attached to flexible PVC tubing that was extended on a rigid PVC pole close to the center/main flow of the river and lowered to ~1 m below the surface or approximately half way between the water surface and the channel bed where the depth was less than 1 m. Before recording field parameter data and collecting surface water samples, the tubing was flushed with at least four times the tubing volume. Following flushing, field parameters, including SpC, pH, dissolved oxygen (DO), oxidation reduction potential (ORP), and temperature were measured with a calibrated YSI multiprobe model 556 placed in a free-flow cell until all field parameters stabilized (± 5.0 % for SpC, ± 0.2 for pH, ± 20 % for DO, and ± 0.2 °C for temperature).

Water samples for inorganic carbon concentration and C stable isotope analyses were collected unfiltered, in glass vials leaving no airspace, and immediately preserved with $HgCl_2$. Previous tests showed that sample filtration did not change inorganic carbon concentrations or isotope ratios (Jin 2012), and thus can be considered to represent dissolved inorganic carbon concentrations. All other samples were filtered in the field with 0.45 µm pore size in-line, trace-metal grade, canister filters. Samples for DOC analysis were collected in 40 mL amber glass vials that had been pre-combusted (450 °C, 4 h) and immediately preserved with 1 M HCl to a pH 3. Samples for spectrometric analysis were also collected in the same amber glass vials but with no addition of preservative. Samples for anion and alkalinity (Alk) analysis were collected filtered in high density polyethylene bottles with no preservatives added. Samples for cation analysis were collected filtered in 20 mL acid-washed bottles and preserved with trace-metal grade nitric acid to a pH < 2. All the samples were stored on ice and in the dark until delivered to the laboratory. In the laboratory, samples for nutrient analysis were frozen and all other samples were refrigerated (4 °C) prior to analysis.

Laboratory analyses

Aqueous DOC concentrations were measured on a Shimadzu TOC-5000A total organic carbon analyzer. Three to five injections of a 60 µL sample were measured. Only data with <5 % coefficient of variance were accepted and analytical precision was ±0.2 mg L^{-1}. The DIC concentrations were measured by acidifying to release CO_2 which was quantified on an automated coulometer (UIC). Stable C isotopic ratio of the DIC ($\delta^{13}C_{DIC}$) was measured using a ThermoFinnigan MAT 252 mass spectrometer. Isotopic results are expressed in standard delta notation relative to Vienna Peedee Belemnite. Analytical precision based on replication of standards was ± 0.1 %.

Spectrophotometric characteristics, or 3-D excitation-emission matrices (EEMs), of the NDOM were examined using a fluorescence spectrometer (Hitachi F-7000). Spectrophotometric samples were kept in the dark before measurement and analyzed at room temperature. Excitation wavelengths were measured from 200 to 400 nm at 10 nm intervals and emission wavelengths from 200 to 600 nm at 3 nm intervals. The Raman peak intensity of DI water at excitation wavelength 348 nm was used as a standard to monitor instrumental drift. Fluorescence intensity is represented in arbitrary units.

Two spectrometric indices were used to indicate the quality and origin of NDOM. The fluorescence index (FI), defined as

$$FI = \frac{I_{EX=370,\,EM=450}}{I_{EX=370,\,EM=500}} \quad (1)$$

in which I is the intensity at the subscripted excitation/emission pair, provides a metric representing the degree of NDOM aromaticity. It has been used to distinguish between NDOM of terrestrial/soil origin (indicated by a low FI, <1.4) and NDOM of microbial origin (indicated by a large FI, >1.9, McKnight et al. 2001). The humification index (HIX), defined as

$$HIX = \frac{\sum I_{EX=245,\,EM=435\rightarrow480}}{\sum I_{EX=245,\,EM=300\rightarrow345}} \quad (2)$$

provides an indicator of NDOM age and recalcitrance. An HIX < 5 suggests fresh NDOM, derived perhaps from aquatic production, while an HIX > 10 may indicate humified NDOM (Ohno 2002; Zsolnay et al. 1999).

Major ions (F^-, Cl^-, Na^+, K^+, Ca^{2+}, Mg^{2+}, and SO_4^{2-}) were measured using an automated Dionex DX500 ion chromatograph. Samples were titrated and measured for alkalinity at room temperature within 24 h of sample collection. The relative standard

deviation of internal standards measured along with the samples was <3 %. Charge balance errors were <5 % in 48 out of 63 samples. Saturation indices with respect to calcite and dolomite ($SI_{calcite}$ and $SI_{dolomite}$, respectively) were calculated using the geochemical code PHREEQCI (Version 2.18.3-5570) and are given as:

$$SI = \log\left(\frac{IAP}{K}\right) \quad (3)$$

where IAP is the ion activity product and K is the equilibrium constant for a given mineral. Partial pressure of CO_2 (P_{CO2}) for each sample collected was calculated using PHREEQCI.

Hydrologic conditions

Rainfall data were obtained from Suwannee River Water Management District (SRWMD) Water Data Portal (http://www.srwmd.state.fl.us/index.aspx?nid=345). Rainfall for each sampling site was assigned to the nearest SRWMD rainfall station(all within 1 mile), which for sites 700, 2,500, 2,700 and 2,800 were rain stations #79, #212, #241 and #233, respectively (Fig. 1). Rainfall at station #235 was used for sites 1,000 and 1,500, and rainfall at station #240 for the River Sink and Rise. Discharge at the six USGS gauge stations were obtained from the USGS website (http://waterdata.usgs.gov/fl/nwis/rt). At the River Rise and River Sink, discharges were calculated from stage data (obtained from http://www.srwmd.state.fl.us/index.aspx?nid=345) using rating curves developed by Screaton et al. (2004) for the River Rise, and the SRWMD for the River Sink (Rating No.9 for Station Number 02321898, Santa Fe River at O'Leno State Park). Daily water discharge at each site was multiplied by DOC and DIC concentrations at that site in order to calculate the daily river export of DOC and DIC, respectively.

Results

Hydrologic conditions

During the study period (June 2010 to May 2011), the discharge of the Santa Fe River at sites 1,000 and 2,800 ranged from 0.0 to 4.2 $m^3\ s^{-1}$ (mean = 0.4 $m^3\ s^{-1}$) and 25.7 to 42.5 $m^3\ s^{-1}$ (mean = 32.8 $m^3\ s^{-1}$), respectively (Fig. 2). The river discharges at River Rise increased following precipitation with about a 1–3 day lag. No major flooding occurred on the river during the sampling period and river flow varied between about the 20th and 50th percentile of its 10 year average flow. For the purposes of this study, eight sampling events were binned into periods of 'average flow' (Jun-10, Jul-10 and Sep-10), 'low flow' (Feb-11 and Mar-11), and 'very low flow' (Oct-10, Dec-10 and May-11) (Fig. 2). Specifically, the binning was based on river discharge at site 2,800, which captures flow from the entire watershed. Periods with discharge at site 2,800 within the ± 2 $m^3\ s^{-1}$ of 42 $m^3\ s^{-1}$, which is the 10 year average flow at site 2,800, were defined as 'average flow' conditions. Periods with discharge between 30 and 40 $m^3\ s^{-1}$ were defined as 'low flow' conditions, while those with discharge less than 30 $m^3\ s^{-1}$ were defined as 'very low flow' conditions. Based on this criterion, the flow of Santa Fe River is average 14.1 % of the time from May 2001 to May 2011. For 21.7 and 27.0 % of the same time period, the flow of the river can be categorized as low flow and very low flow, respectively. Major flood events (defined as discharge at site 2,800 > 100 $m^3\ s^{-1}$) occurred seven times from May 2001 to May 2011 and account for the 1.9 % of the time and the remainder of the time, the river was not flooding, but above average flow. None of these times of elevated flow was sampled.

Variations in DOC and DIC with flow

Concentrations of DOC decreased downstream while the DIC concentration increased downstream, resulting in a statistically significant inverse relationship ($p < 0.0001$) between their concentrations (Fig. 3). The DOC concentrations in the upper watershed ranged from 2.5 to 63.4 mg L^{-1} (mean = 21.8 ± 16.6 mg L^{-1}, $n = 32$). These values are significantly greater ($p < 0.001$) from those in the lower watershed, which ranged from 0.0 to 44.0 mg L^{-1} (mean = 6.0 ± 9.0 mg L^{-1}, $n = 31$). At all sampling sites, DOC concentrations were greatest during times of average flow (Fig. 3). In the upper watershed, DOC concentrations ranged from 12.4 to 63.4 mg L^{-1} (33.5 ± 18.3 mg L^{-1}, $n = 12$) during average flow, from 17.6 to 32.7 mg L^{-1} (26.4 ± 4.9 mg L^{-1}, $n = 8$) during low flow, and from 2.5 to 15.3 mg L^{-1} (6.9 ± 4.0 mg L^{-1}, $n = 12$) during very low flow. In

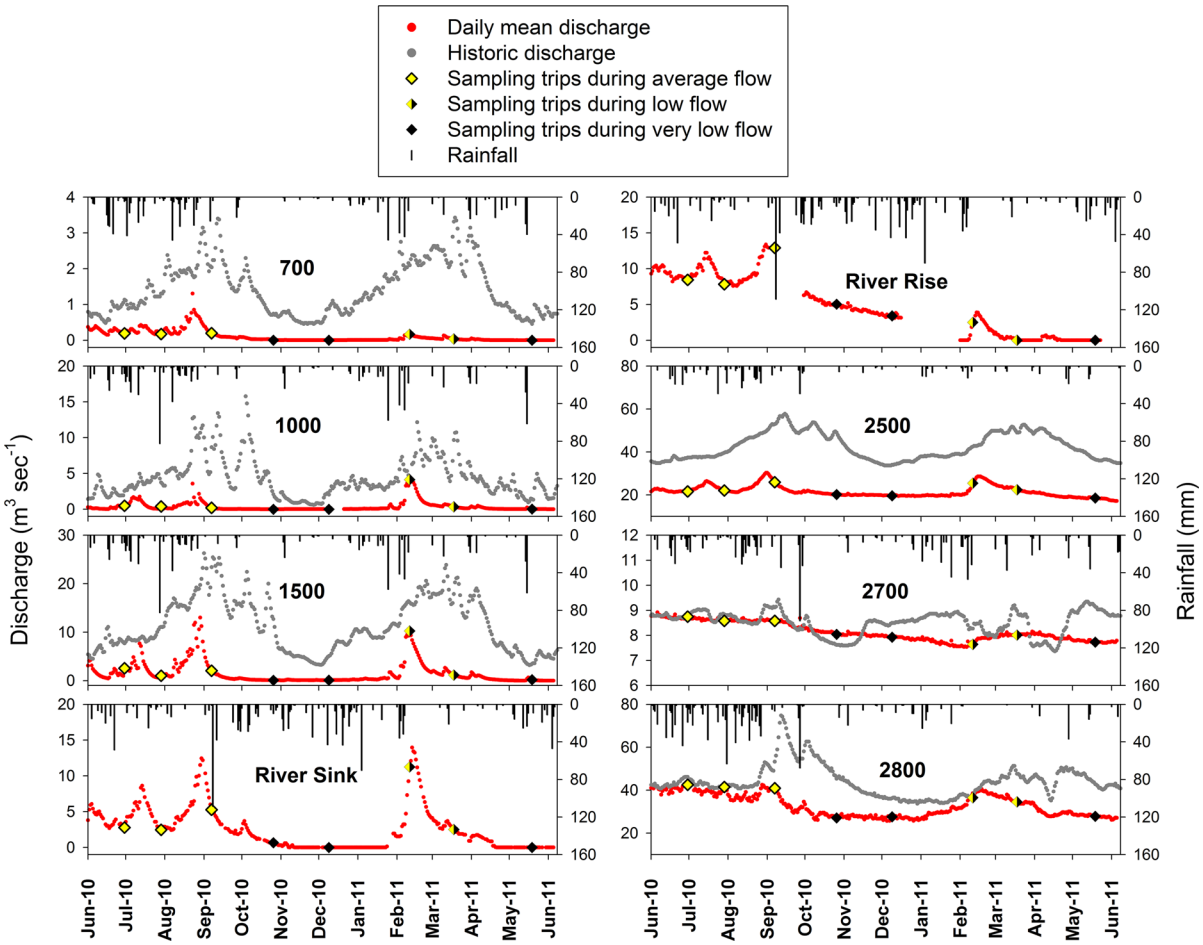

Fig. 2 Hydrologic condition of the Santa Fe River watershed during the study period. Daily mean (*red points*) and historic mean (*grey points*, calculated for about 50-year of data) discharge (in m3 sec-1) of the Santa Fe River at the eight sampling sites and rainfall data recorded at nearby SRWMD stations. The River Rise and River Sink do not have long term records of flow. Each sampling period is designated as either average, low or very low flow (*yellow*, *half-yellow* or *black diamonds*, respectively). (Color figure online)

the lower watershed, DOC concentrations varied similarly with flow, ranging from 0.1 to 44.0 mg L^{-1} (10.5 ± 12.9 mg L^{-1}, $n = 11$) during average flow, from 0.8 to 18.5 mg L^{-1} (6.7 ± 6.3 mg L^{-1}, $n = 8$) during low flow, and from 0.0 to 5.0 mg L^{-1} (1.5 ± 1.3 mg L^{-1}, $n = 12$) during very low flow.

The slope of the inverse relationship between DIC and DOC became more negative as river flow decreased, reflecting large decreases in DOC concentrations and small increases in DIC concentrations with decreasing river discharge (Fig. 3). The DIC concentrations in the upper watershed ranged from 1.5 to 40.9 mg L^{-1} (16.5 ± 12.3 mg L^{-1}, $n = 32$), and were significantly ($p < 0.001$) lower than in the lower watershed, where concentrations ranged from 9.0 to 40.8 mg L^{-1} (32.4 ± 7.2 mg L^{-1}, $n = 31$). In contrast to DOC, the DIC concentrations were greatest during very low flow. In the lower watershed, DIC concentrations averaged 28.4 ± 7.6 mg L^{-1} ($n = 11$) during average flow, 31.0 ± 7.9 mg L^{-1} ($n = 8$) during low flow, and 37.1 ± 2.6 mg L^{-1} ($n = 12$) during very low flow.

During most sampling periods, DOC export generally increased downstream, even during very low flow conditions (Fig. 4), implying a source of dissolved OM in the lower watershed, although only small amounts. The DOC increased least during very low flow, and elevated amounts of DOC were exported during low and average flow. During the two low flow periods measured, DOC export dropped between the

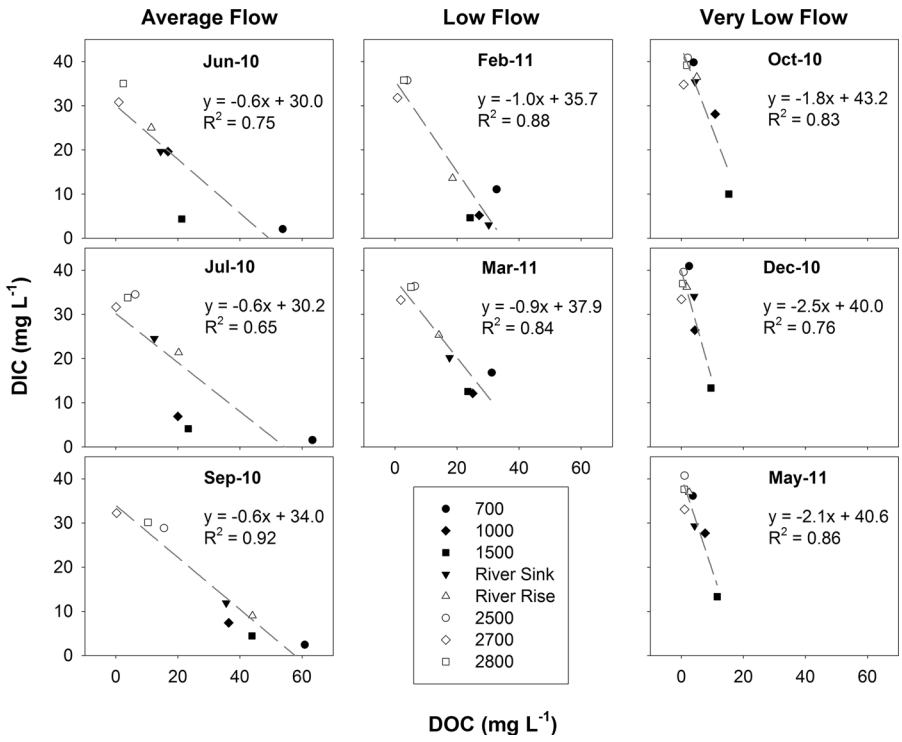

Fig. 3 Relationship between DIC and DOC concentrations in water samples collected from the upper and lower Santa Fe River watershed (closed and open symbols, respectively) during average, low and very low flow conditions (in columns left to right). Dashed lines and the equations indicate the linear regression of the DIC-DOC relationship

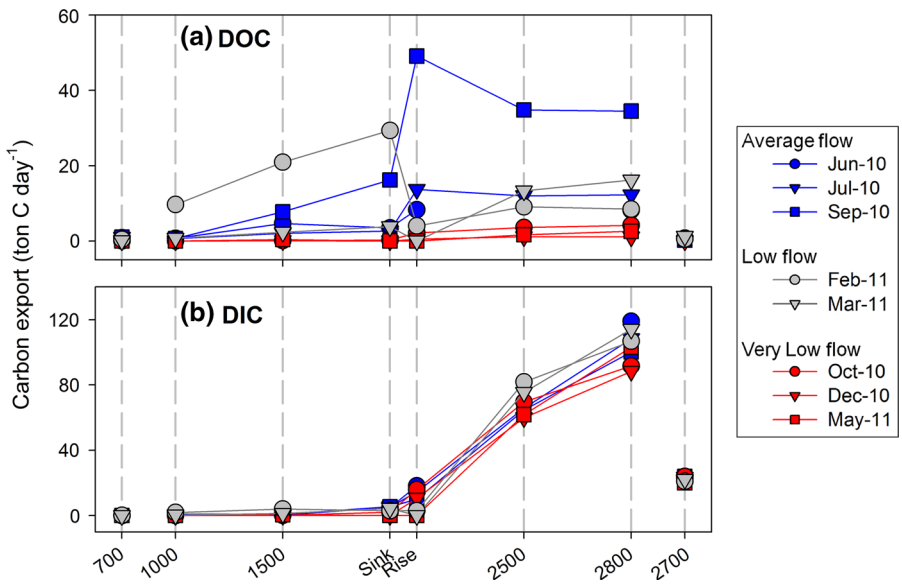

Fig. 4 Riverine carbon exported from each sampling site in the Santa Fe River watershed during average (*blue*), low (*grey*) and very low flow (*red*) conditions. Spacing on the x-axis scale represents river distance between sampling sites. (Color figure online)

River Sink and the River Rise, reflecting a loss of DOC, but at average flow the DOC increase between the River Sink and Rise.

Export of DIC varied little with flow condition and was low throughout the upper watershed (Fig. 4). Below the River Sink, DIC increased progressively with the greatest increase occurring between the River Rise and site 2,500, the portion of the river with the most springs. These data show the predominant source of DIC to be groundwater, delivered to the river via springs in the lower watershed equally during all flow conditions (Khadka et al. 2014).

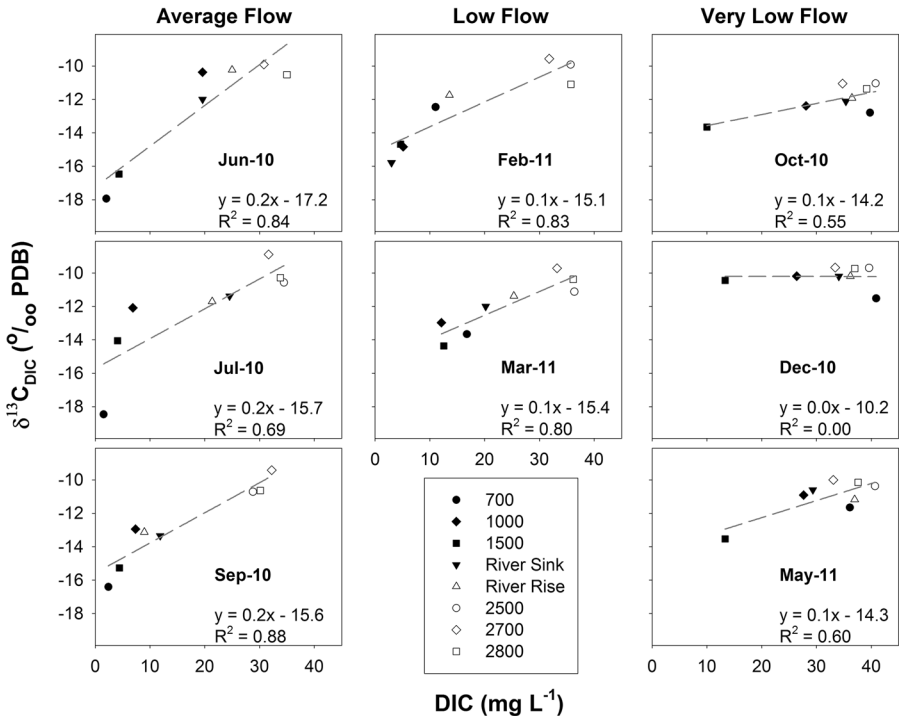

Fig. 5 Relationship between d13CDIC and DIC concentrations among water samples collected from both the upper and lower Santa Fe River watershed (closed and open symbols, respectively) during average, low and very low flow conditions (columns left to right). Dashed lines and equations show the linear regression of the DIC-d13CDIC relationship

Stable carbon isotopic variations

DIC concentrations were linearly correlated with the $\delta^{13}C_{DIC}$ values (Fig. 5). the $\delta^{13}C_{DIC}$ values ranged from -18.5 to -10.2 ‰ (mean $= -13.2 \pm 2.2$ ‰, $n = 32$) in the upper watershed and were significantly ($p < 0.001$) lower and more variable than those in the lower watershed, which ranged from -13.1 to -8.9 ‰ (mean $= -10.6 \pm 0.9$ ‰, $n = 31$). The lowest $\delta^{13}C_{DIC}$ values occurred during very low flow and the highest values occurred during average flow. These data are consistent with a depleted source of DIC in the upper watershed, possibly from respired OM and an enriched source in the lower watershed, possibly from the carbonate rock in the Floridan aquifer ($\sim$0 ‰, Clark and Fritz 1997; Khadka et al. 2014; Randazzo and Jones 1997).

NDOM spectophotometric characteristics

Variations in the quality of NDOM through the Santa Fe River watershed and over time were indicated by spectophotometric characteristics of the water samples. EEMs for all the samples collected are presented in the Supplementary Section. Most water samples had broadly similar EEMs that contained both humic-like (A, excitation/emission wavelengths: 210–260/410–450 nm) and fulvic-like (C, 310–340/410–420 nm) fluorophores. In addition, most samples exhibited two relatively weak protein-like fluorophores (T1, 275–280/340–360 nm and T2, 215–220/310–340 nm). However, the spectrometric indices showed systematic trends in NDOM quality not apparent in the EEMs alone (Fig. 6). NDOM in the upper-most river water (700) had the greatest aromaticity and recalcitrance (FI and HIX index, respectively) during average flow conditions, approaching that of a humic acid standard (Sigma-Aldrich, CAS#: 1415-93-6). While all river samples had NDOM spectrometric signatures indicative of humified OM, riverine NDOM became more labile and less aromatic (increasing FI and decreasing HIX index, respectively) downstream and with decreasing flow. This relationship suggests that progressively increasing OM additions to the river during increased flow occurred from either microbial or algal sources, particularly during very low flow conditions.

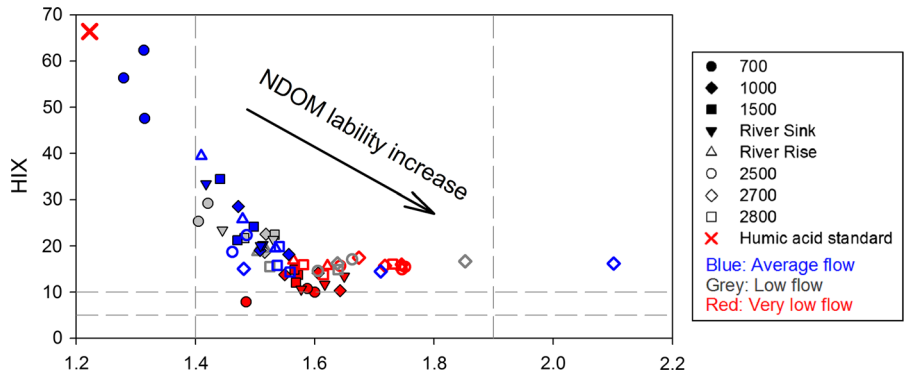

Fig. 6 Relationship between two fluorescence indices, FI and HIX, for water samples collected from both the upper and lower Santa Fe River watershed (closed and open symbols, respectively) during average (*blue*), low (*grey*) and very low flow (*red*) conditions. (Color figure online)

Variations in major ion concentrations and other water chemistry parameters

Only some of the major ion concentrations and other water chemistry parameters measured in the water samples varied spatiotemporally (Table S1). Concentrations of Ca^{2+} and Mg^{2+} throughout the watershed as well as concentrations of SO_4^{2-} in the lower watershed decreased from very low to average flow conditions. Concentrations of Ca^{2+} and SO_4^{2-} were also greater in the lower than upper watershed. The pH of the river water was close to neutral, but slightly more basic in the lower watershed. During higher flow periods, the Santa Fe River water generally had greater ORP but lower DO, Alk, and SpC, especially in the lower watershed.

Discussion

Much of the chemical variations in Santa Fe River may reflect influx of soil water and dilution by groundwater depending on flow characteristics, but the system may also be influenced by additional water sources and in situ biogeochemical processes. To examine these processes, a mixing model previously developed for the Santa Fe River Sink-Rise system (Jin et al. 2014) was applied to the entire watershed. The difference between model and observed concentrations results were used to assess biogeochemical reaction and their controls on the water chemistry.

Three end member water sources were previously identified in the Santa Fe Sink-Rise system, including soil water, groundwater and the deep aquifer (Jin et al. 2014; Moore et al. 2009).The soil water end member is DOC-rich and DIC-poor, with low $\delta^{13}C_{DIC}$ values and is likely derived from wetlands perched on the Hawthorn Group confining unit. The groundwater end member is DOC-poor and DIC-rich with high $\delta^{13}C_{DIC}$ values. This end-member is most common in the lower watershed and during very low flow periods, reflecting its origin from springs discharging from the UFA. The deep aquifer groundwater end member represents a small fraction of the total river discharge (at most 24 %) and has DOC and DIC concentrations similar to the main groundwater end member but with a heavier $\delta^{13}C_{DIC}$ signature and significantly higher ion concentrations (e.g., SO_4^{2-}, Ca^{2+} and Mg^{2+}), SpC and temperature (Moore et al. 2009). Moore et al. (2009) identified this water as having upwelled from several hundred meters depth in the aquifer. Its enriched composition may be due either to evaporite dissolution or to microbial processes as has been discussed elsewhere (Jin et al. 2014; Moore et al. 2009).

The model used concentrations of Na^+, Cl^- and SO_4^{2-}, shown to be conservative species in this system (Jin et al. 2014; Moore et al. 2009), to define the three end members and to calculate the proportions of water from each source in each sample. The soil water end member composition was chosen to be that of water collected from site 700 on Jul-10 (average flow), because this sample showed the lowest DIC, the highest DOC and the lightest $\delta^{13}C_{DIC}$ value among all samples collected during the 1 year sampling period. The groundwater end member was represented by water collected from site 2,700 on the Ichetucknee spring run on Dec-10 since it was one of the lowest flow periods and displayed the lowest Na^+ and Cl^- concentrations as well as the second heaviest $\delta^{13}C_{DIC}$ value among all samples. The deep water end member was defined by water collected at ~30 m depth from a groundwater

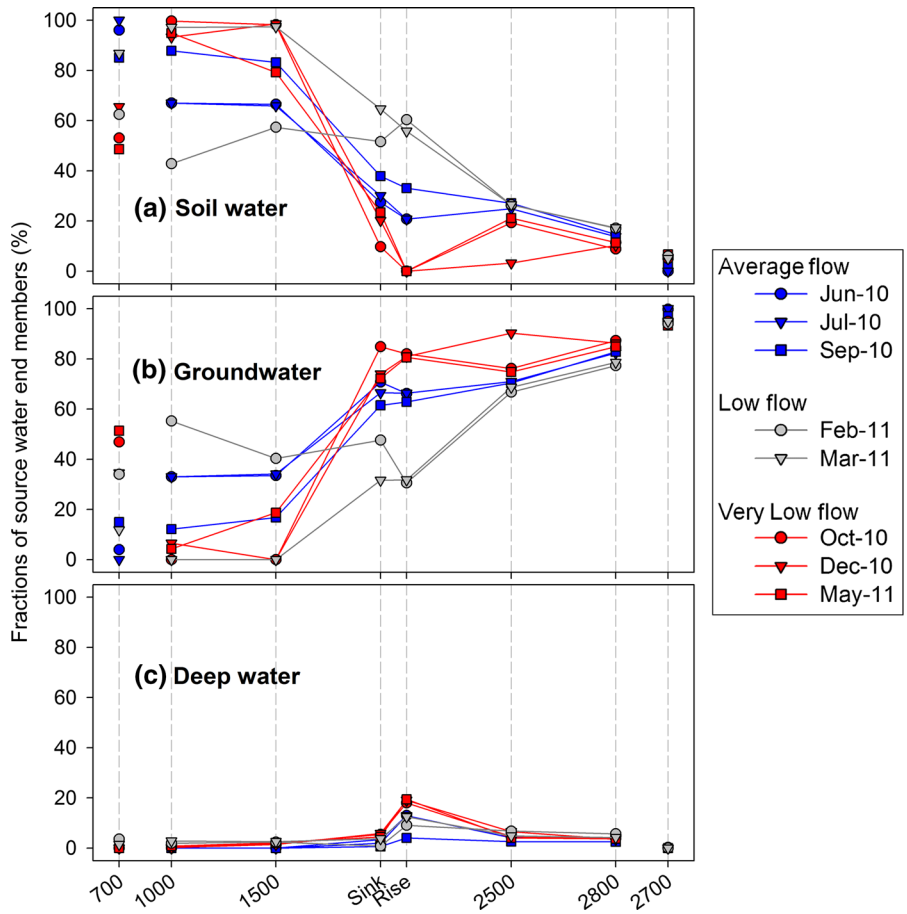

Fig. 7 Results of the water source mixing model shown as the fractions (in %) of **a** soil water, **b** groundwater, and **c** deep water theoretical endmember water sources in each sample collected at each of eight sites during average (*blue*), low (*grey*), and very low (*red*) flow conditions. Spacing on the x-axis scale represents river distance between sampling sites. (Color figure online)

monitoring well located ~2 km southwest of the River Sink on 1/17/2007 as this sample had the highest total inorganic ion concentrations among many wells monitored in the region from 2003 to 2007 (Jin et al. 2014; Moore et al. 2009). Additional details on these samples are provided in Supplemental Table S2.

The model calculates the proportion of each of the three end member source waters in each sample using a mass-balance approach that assumes:

$$f_{soil} + f_{gw} + f_{deep} = 1, \quad (4)$$

$$SO4_n = f_{soil}SO4_{soil} + f_{gw}SO4_{gw} + f_{deep}SO4_{deep}, \quad (5)$$

$$Na_n = f_{soil}Na_{soil} + f_{gw}Na_{gw} + f_{deep}Na_{deep}, \quad (6)$$

$$Cl_n = f_{soil}Cl_{soil} + f_{gw}Cl_{gw} + f_{deep}Cl_{deep}, \quad (7)$$

where f is the volumetric fractions of three endmember, 'soil', 'gw' and 'deep', representing soil water, groundwater and deep water, respectively. $SO4_n$, Na_n and Cl_n are the concentrations of SO_4^{2-}, Na^+ and Cl^-, respectively, in any given water sample n. These equations were solved iteratively and simultaneously using Microsoft Excel's Solver add-in function by minimizing the residuals of solutions to Eqs. 4–7.

All water samples were composed largely of the soil and groundwater end members, the former generally decreasing and the latter increasing with distance downstream (Fig. 7). In the upper watershed (sites 700, 1,000 and 1,500), the soil water end member represented an average of 79 % (ranging 43–100 %) of the water samples collected, while the groundwater end member provided 85 %, on average (ranging 67–100 %) of the samples collected in the lower watershed. The shift from samples composed predominately of soil water to predominantly groundwater occurred between 1,500 and the Sink. Only samples collected near the Sink-Rise region of the watershed had significant contributions from the deep groundwater end member.

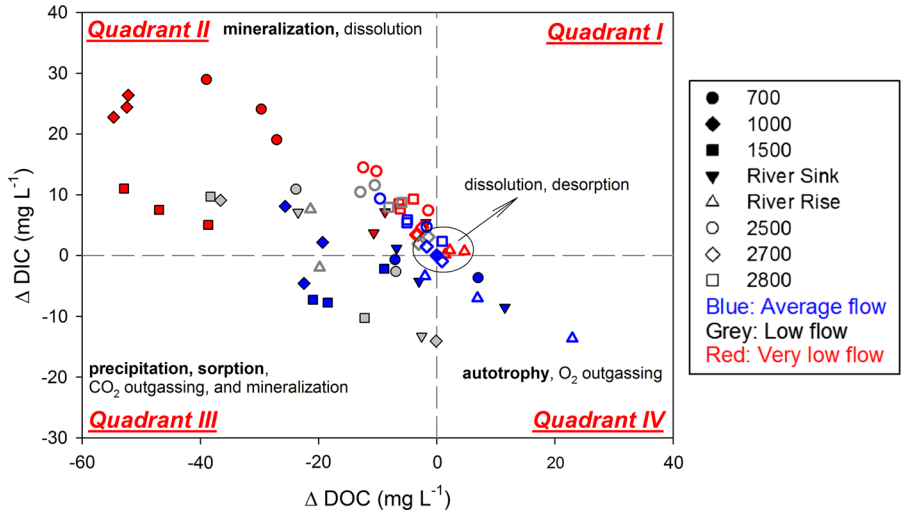

Fig. 8 Differences between the model-predicted and measured dissolved inorganic carbon and organic carbon concentrations (ΔDIC and ΔDOC, respectively) in samples from the upper and lower Santa Fe River watershed (closed and open symbols, respectively) during average, low and very low (*blue*, *grey*, and *red*, respectively) flow conditions. Possible biogeochemical processes responsible for differences are listed in each quadrant, with the hypothesized dominant ones in bold font. (Color figure online)

Simplifying assumptions of the mixing model include (1) no more than three chemically distinct sources of water occur in the system, (2) Na^+, Cl^- and SO_4^{2-} behave conservatively in the system, and (3) the Na^+, Cl^- and SO_4^{2-} concentrations of the three samples used to represent the end members have pure end member compositions. To evaluate the effects of violations of these assumptions, a series of sensitivity analyses were performed in which mixing proportions were recalculated after altering each ion concentration by one standard deviation of its variance in the system. These tests resulted in changes in the volumetric mixing fraction of each end member was only 3.5, 4.9 and 3.8 %, on average, for Na^+, Cl^- and SO_4^{2-}, respectively. This sensitivity affected each end member source equally and there was no apparent directional bias in the model results.

Spatiotemporal distribution of biogeochemical processes

The biogeochemical processes that may occur both in the groundwater and surface water in the Santa Fe River system have recently been discussed for the area around the Sink-Rise system, where groundwater and surface water interactions are most intense (Jin et al. 2014). Similar to results presented in Jin et al. (2014), differences between the mixing model and observed results is reported as Δ values, which are positive when reactions provide sources and negative when reactions consume dissolved components from the water (Table S3).

The results of these calculations for the C system are shown in a plot of ΔDIC versus ΔDOC values for all water samples (Fig. 8). Most samples plot in Quadrant II, indicating they have lost DOC, perhaps through mineralization or NDOM-mineral desorption, and gained DIC through either mineralization of NDOM or carbonate mineral dissolution or both. Water in our study area is unlikely to have gained DIC from the atmosphere since the watershed was supersaturated with respect to atmospheric CO_2 ($\log P_{CO2} = -2.4 \pm 0.5$ atm). Many samples plot in Quadrant III indicating they have lost both DOC and DIC, perhaps through autotrophy, carbonate precipitation, degassing to the atmosphere or all three. A similar approach was used to examine biogeochemical influence on other species and produce graphs of ΔDO–ΔDOC (Fig. S8), ΔDIC–ΔCa (Fig.S9), and ΔDIC–$\Delta\delta^{13}C_{DIC}$ (Fig. S11), which are used below to examine the distribution of each biogeochemical process.

The robustness of the results (Δ values) was tested using the model sensitivity analysis described

previously. Variations in the end member source water mixing fractions caused by a one standard deviation change in the ion concentrations defining each end member resulted in changes in ΔDIC and ΔDOC values of <3and <5 mg/L, respectively for upper watershed samples, and <2 and <1 mg/L, respectively for lower watershed samples. These values are small compared to the range of the calculated chemical effects of biogeochemical processes.

Mineralization of NDOM

Samples falling within Quadrant II of Fig. 8 are likely to have been altered through mineralization of NDOM. Most of these samples (30 out of 40) also showed oxygen consumption (mean $\Delta DO = -0.7 \pm 1.8$ mg L^{-1}, Fig. S8) and DOC loss was stoichiometrically similar to DIC produced (ΔDOC: ΔDIC ~ -1, Fig. 8). Consumption of DO is smaller than the amount of DOC lost (Fig. S8), other oxidants may have provided terminal electron acceptors or DOC may have sorbed to mineral surface. The negative ΔDOC values in Quadrant III of Fig. 8 also suggest mineralization of NDOM. This inference is supported by most of the samples which exhibiting negative ΔDO values (-0.8 ± 2.1 mg L^{-1}) and have the lightest $\delta^{13}C_{DIC}$ values (-14.0 ± 2.3 ‰) among all samples collected.

The greatest net NDOM loss occurred during very low or low flow conditions and mainly in the upper watershed (Fig. 8). This pattern may result from slower water flow in the upper watershed that allows more time for heterotrophic microbes to respire NDOM and for biogeochemical products such as DIC and H^+ to accumulate. Alternatively, greater net heterotrophy of the upper watershed may relate to lower autotrophic production in this portion of the river, as a consequence of the lower water temperatures, lower nutrient concentrations and less light penetration (i.e. UV light absorbing, Laurion et al. 1997; Morris et al. 1995)found there relative to the lower watershed.

Most samples had negative ΔDOC indicating that NDOM was lost throughout the watershed. Though humic substances, which are abundant in the NDOM of blackwater systems such as the Santa Fe River, are usually considered refractory, this finding is consistent with the fact that most inland aquatic ecosystems are net heterotrophic (Wetzel 2001). The spectrophotometric data show that most of the NDOM is a mixture of fresh and humified materials of both plant and microbial origin (Fig. 6). Mineralization of NDOM has been noted to occur in several other karst subsurface (Hancock et al. 2005; Kortelainen and Karhu 2006; McMahon 2001; Pronk et al. 2006) and blackwater river systems (Benner et al. 1995; Meyer et al. 1987; Moran et al. 1999; Petrone et al. 2011).

Autotrophic production

Only five samples plot in Quadrant IV of Fig. 8, with positive ΔDOC and negative ΔDIC values, suggesting net autotrophic production. The occurrence of autotrophic production in these samples is supported by an increase in their NDOM lability ($\Delta FI = 2.3 \pm 3.3$ and $\Delta HIX = -0.4 \pm 0.2$, Table S3), but contradicted by their negative ΔDO values. While net autotrophic production is not apparent in most samples collected, it still likely occurred, just to a lesser extent than NDOM mineralization. The imprint of autotrophic processes may be found in the higher redox values during the summer (ORP = 215.1 ± 64.6 mV vs. 160.4 ± 123.6 mV during winter, $p = 0.11$) with elevated solar radiation and observations of an inverse correlation between DO and nitrate removal in the Ichetucknee River (Heffernan et al. 2010). The autotrophs were not necessarily phytoplankton as algal biomass was low throughout the system (chlorophyll-a concentrations < 0.3 mg L^{-1}, data obtained from STORET Data Warehouse http://www.epa.gov/storet). Instead, photosynthesis by subaquatic vegetation maybe of greater importance, as mats of tapegrass (*Vallisneria americana*) and eelgrass (*Sagittaria kurziana*) cover up to 78 % of the surface of the river bed in some Florida springs (Canfield and Hoyer 1988; Kurz et al. 2004). Previous studies have measured high benthic production in Florida springs (Heffernan et al. 2010; Saunders et al. 2007), which also suggests that subaquatic vegetation are the main autotrophic producers.

Dissolution of carbonate

Samples showing evidence of carbonate mineral dissolution were distributed similarly to those marked by NDOM mineralization. For instance, the occurrence of carbonate dissolution in samples in Quadrant II of Fig. 8 is supported by their positive ΔCa (0.3 ± 0.2 mg L^{-1}), ΔMg (0.3 ± 0.1 mg L^{-1}),

ΔSpC (87.7 ± 41.4 μS cm^{-1}), and ΔDIC values (9.6 ± 5.6 mg L^{-1}). Further, $\delta^{13}C_{DIC}$ values were isotopically heavier than expected from mixing alone ($\Delta\delta^{13}C_{DIC} = 3.7 \pm 2.3$ %, Fig. S11). Organic mineralization, which releases protons from the dissociation of the C compounds it liberates, has been suggested to drive carbonate dissolution (Alberic and Lepiller 1998; Li et al. 2010).

Small positive ΔSpC, ΔCa, ΔMg and ΔpH are found in samples in Quadrant I and others close to the origin in Fig. 8 (and Table S3), suggesting that these samples may also have experienced some degree of carbonate dissolution. It is not surprising that these samples were largely collected from the River Rise or site 2,700 during very low or low flow conditions as this is where and when samples would be expected to be composed of water newly emerged from the subsurface, thus reflecting carbonate dissolution that occurred in the aquifer.

Precipitation of carbonate

Samples plotting in Quadrant III of Fig. 8, which show DIC consumption (negative ΔDIC), also generally have negative ΔCa (Fig. S9), positive ΔpH values as well as negative ΔAlk and ΔSpC values (Table S3), all suggesting carbonate mineral precipitation. However, the majority of those samples were calculated to be undersaturated with respect to carbonate minerals. Alternatively, SI calculation may not be reliable because concentrations of PO_4^{3-} were not taken into consideration. Most of the samples of Quadrant III were collected in the upper watershed where elevated phosphorus concentrations have been found (Katz 1992). We assume the concentrations to be $\sim$0.8 mg L^{-1} based on other north Florida rivers (SRWMD Water Data Portal, http://www.srwmd.state.fl.us/index.aspx?nid=345). Inclusion of this average PO_4^{3-} concentration into the SI calculation shifts the average SI increase to 1.7 and, thus, shift the saturation state to supersaturated with respect to calcite.

NDOM-mineral sorption and desorption

NDOM concentrations may drop for samples plotting in Quadrant III of Fig. 8 through sorption to carbonate mineral surfaces. (Frye and Thomas 1993; Jin and Zimmerman 2010; Thomas et al. 1993). In addition, positive ΔpH values in the majority of these samples (mean $\Delta pH = 0.52 \pm 0.52$) may be partly attributed to NDOM-mineral sorption, since carbonate minerals have been previously reported to preferentially sorb acidic NDOM groups and thereby increase solution pH (Jin and Zimmerman 2010).

On the other hand, NDOM-mineral desorption may be common in the Santa Fe River watershed, as most of the samples collected were found to have experienced carbonate dissolution. A linkage between carbonate dissolution and NDOM-mineral desorption has been reported previously in laboratory experiments using UFA rocks (Jin and Zimmerman 2010) as well as in field investigation of the Santa Fe River Sink-Rise system (Jin et al. 2014). In addition to increasing DOC concentrations, NDOM desorption has been found to alter NDOM quality (Jin and Zimmerman 2010).

Relative magnitudes of biogeochemical processes

The results of the model (Δ values) only provide information on the net effects of simultaneously occurring biogeochemical processes. The relative magnitude of each process may be assessed by assuming reaction stoichiometries for each process. First, using ΔCa values, we estimate the amount of DIC that would have been released or consumed via carbonate mineral dissolution or precipitation, respectively, by assuming a DIC:Ca molar ratio of 1:1, expected from congruent calcite dissolution. Next, DOC consumed or released or sorbed during carbonate dissolution or precipitation, respectively, was calculated by assuming a ratio of 8.0 mg DOC kg^{-1} rock (or a DOC:Ca molar ratio of 6.7×10^{-5}), derived from desorption experiments using Floridan aquifer materials Jin and Zimmerman (2010). Lastly, changes in DIC and DOC attributable to mineralization or autotrophy were calculated as that portion of ΔDIC and ΔDOC as yet unaccounted for by the above reactions. These calculations can be expressed as:

$$\Delta DIC_{diss./precip.} = \Delta Ca \quad (8)$$

$$\Delta DIC_{auto./resp.} = \Delta DIC_{total} - \Delta DIC_{diss./precip.} \quad (9)$$

$$\Delta DOC_{desorb/sorb} = 6.7 \times 10^{-5} \times \Delta Ca \quad (10)$$

$$\Delta DOC_{auto./resp.} = \Delta DOC_{total} - \Delta DOC_{desorb/sorb} \quad (11)$$

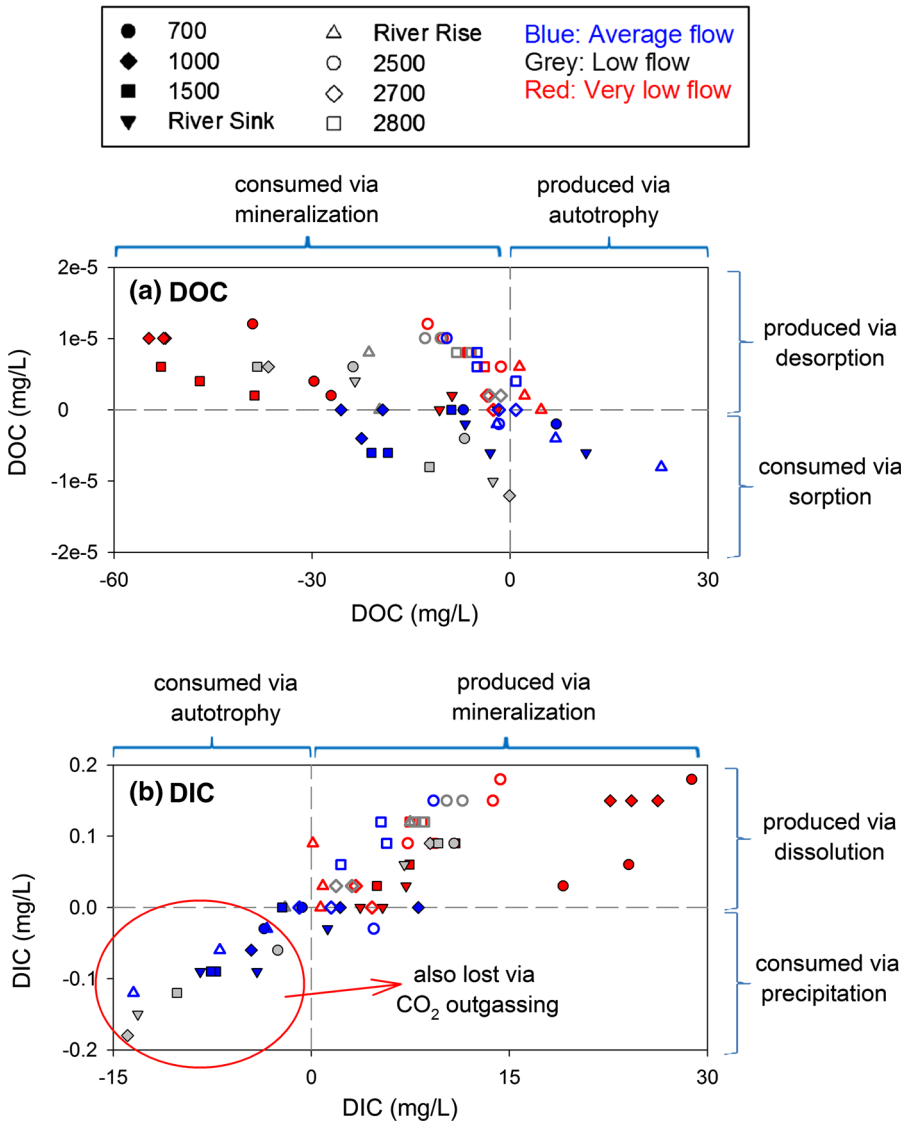

Fig. 9 Effects of various biogeochemical processes on **a** DOC and **b** DIC quantity in samples collected from both the upper and lower Santa Fe River watershed (closed and open symbols, respectively) during average (*blue*), low (*grey*) and very low flow (*red*) conditions. See text for calculation method. (Color figure online)

Given these stoichiometries, our samples were influenced most strongly by mineralization, which consumed DOC at about twice the rate that autotrophy produced it and many times the rates that desorption/sorption or dissolution/precipitation altered DOC concentrations (Fig. 9a). Meanwhile, mineralization produced DIC at rates similar to that of its consumption by autotrophy but many times the rates that desorption/sorption or dissolution/precipitation altered DIC concentrations (Fig. 9b). Rates of NDOM mineralization almost tripled, when the river dropped from average to very low flow.

Biogeochemical processes were more important to river water chemistry in the upper watershed and during very low flow periods than in the lower watershed. On average, hydrologic mixing in the lower watershed induced changes in DOC and DIC concentrations that are approximately ten times those caused by biogeochemical processes. In the upper watershed, biogeochemical processes had a greater

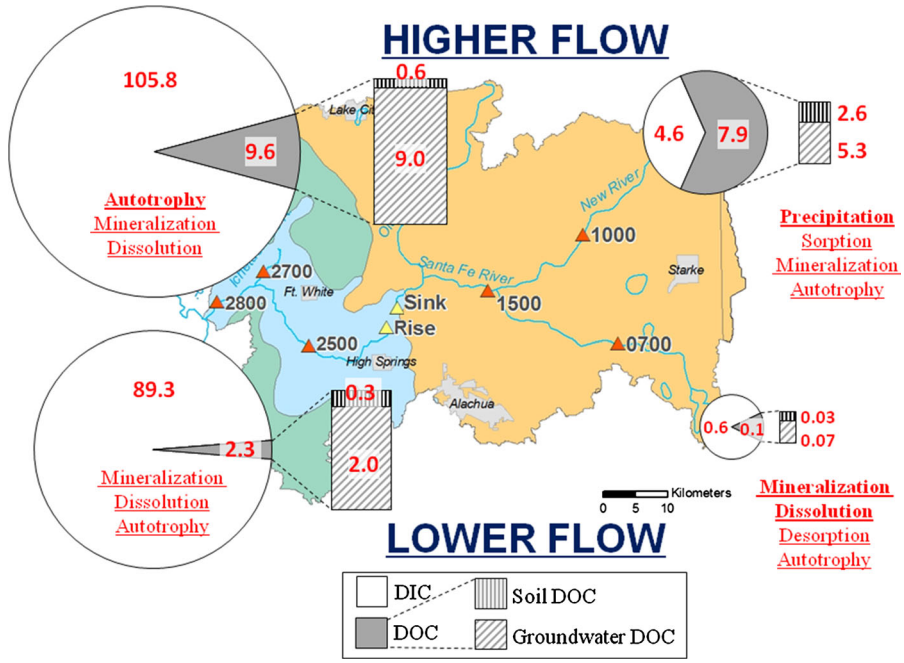

Fig. 10 Average daily carbon export (in metric ton day-1) from the upper and lower watershed (measured as export at the Sink and and export at Site 2800 minus the Sink, respectively), during higher and lower flow periods. Pie charts show distribution of inorganic and organic C and calculated sources. Deduced biogeochemical processes responsible for gain or loss of carbon from each portion of the watershed, with the dominant ones in bold font are also listed. (Color figure online)

influence on C concentrations, producing changes in DOC and DIC that were roughly half to a third those of hydrological mixing. For example, at site 2,800 on Sep-10, biogeochemical processes altered DOC and DIC concentrations by 0.9 and 2.3 mg L^{-1}, respectively, while hydrologic mixing changed DOC and DIC concentrations by 9.4 and 27.8 mg L^{-1}, respectively. On the same day at site 1,000, biogeochemical processes changed DOC and DIC concentrations by 19.3 and 2.2 mg/L, respectively, while mixing changed 55.7 and 5.2 mg/L, respectively. These biogeochemical processes, however, had less influence on measured C variations in the Santa Fe River watershed than did hydrologic mixing. However, it is clear from this study that variations in C dynamics resulting from biogeochemical processes were related to or driven by hydrologic mixing and seasonal variations in watershed hydrology.

Riverine carbon export

To estimate the C export of the Santa Fe River watershed, the 1 year study period was divided into eight time intervals: 5 intervals (191 days) that bracketed average and low flow sampling events and three intervals (174 days) that bracketing only the three very low flow sampling events (Table S4). The C export from each portion of the watershed was then calculated as the sum of products of the DOC or DIC concentration measured during each sampling event, the average discharge for that time period, and the number of days in the time interval.

Regardless of flow, the average daily export of total C and both DIC and DOC was less from the upper watershed, as measured at the River Sink than that from the lower watershed alone, which was calculated as the difference in C flux at site 2,800 and the River Sink (Fig. 10). This larger C flux from the upper watershed occurred even though the lower watershed has a smaller area than the upper watershed (1,065 km^2 vs. 2,520 km^2, respectively). During average and low flow, the average daily export of DIC from the upper and lower watershed was estimated to be 4.6 and 105.8 metric ton day^{-1}, respectively, and 0.6 and 89.3 ton day^{-1} during lower flow, respectively. These results are consistent with a

Table 1 Comparison of DOC and DIC export from selected watersheds

Watershed name	Watershed characteristics	DOC export (ton km^{-2} $year^{-1}$)	DIC export (ton km^{-2} $year^{-1}$)	Reference
Santa Fe River watershed, FL, USA	temperate watershed: karst; forested	1.0	10.3	This study
Santa Fe River watershed, FL, USA	temperate watershed: karst; forested	2.5	10.2	Khadka et al. 2014
6 watersheds in northern Sweden	subarctic watershed: deciduous forest and shrub; underlain mainly by schist and salic igneous rocks	0.8–2.3	1.0–3.3	Giesler et al. 2014
16 watersheds in Finland, Scotland UK	subarctic or temperate watershed; peat-dominated	5–10	NA	Aitkenhead and McDowell 2000 and references therein
Bigelow Brook watershed, MA, USA	temperate watershed: well drained with glacial till derived soil deposits; forested	1.7	NA	Wilson et al. 2013
Raccoon River watershed, IA, USA	temperate watershed; underlain by thick pebbly glacial till	1.2	NA	Jones and Schilling 2012
Penobscot River watershed, ME, USA	temperate watershed: heavily forested	5.8	NA	Cronan 2012
Orinoco River, Venezuela	tropical watershed: floodplain and savanna forests	5.3	NA	Lopez et al. 2012
Yukon River basin, AK, USA	arctic and subarctic watershed	NA	5.2	Guo et al. 2012
Raccoon River watershed, IA, USA	temperate watershed; underlain by thick pebbly glacial till	NA	11.3	Jones and Schilling 2012
Ottawa River Basin, Canada	temperate high latitude watershed; underlain largely by Precambrian granitic rocks	NA	3.5	Telmer and Veizer 1999
Nyong watershed, Cameroon	tropical watershed: underlain primarily by granitoids, gneiss and migmatites	NA	0.9	Brunet et al. 2009

recent study on the Santa Fe River which reported DIC export to be 100.3 ton day^{-1} from June 2010 to August 2012 (Khadka et al. 2014). While it is not surprising that the lower watershed exported so much more DIC than the upper watershed given that most of the DIC originated from carbonate rock-equilibrated groundwater emerging from springs in the lower watershed, it highlights the dominating role of carbonate dissolution over biogeochemical processes such as soil or in situ respiration in DIC production from karstic systems such as the Santa Fe River watershed.

More surprising is that greater amount of DOC originated from the lower versus upper watershed at all times, despite its smaller area. The lower watershed DOC flux was 9.6 ton day^{-1} during higher flow and 2.3 ton day^{-1} during lower flow, while the upper watershed DOC flux was 7.9 ton day^{-1} during higher flow and 0.1 ton day^{-1} during lower flow (Fig. 10). This can be explained by the also unexpected finding that the majority of DOC produced by all portions of the watershed was derived from groundwater. The portion of DOC calculated to be groundwater-derived ranged from 67 % for the upper watershed to 94 % in the lower watershed, both recorded during higher flow conditions. This groundwater DOC, meted out at concentrations often lower than 1 mg L^{-1} (Duarte et al. 2010) may have been produced by subsurface microbes, desorbed from carbonate rock, or be transformed surface-derived NDOM, though it does not appear to be chemically similar to humic acids. A small portion of this DOC may also have also been

produced by autotrophy within springs and rivers of the lower watershed (Jin et al. 2014).

Using this same approach, the Santa Fe River watershed was calculated to export a total of 3,746.8 ton $year^{-1}$ of DOC during the period of this study, which can be considered a conservative value given that the year studied was relatively dry. In another study of the Santa Fe river, annual DOC export was calculated to be 2.5 times greater than our estimate (Table 1), but this included sampling during the 2012 flood event caused by Tropical Storm Debby, which caused discharge at site 2,800 to increase to around 300 m^3 s^{-1} (Khadka et al. 2014). The area-normalized DOC export of 1.0 ton km^{-2} $year^{-1}$, is comparable to that of many arctic or temperate watersheds, but less than many tropical or peat-dominated watersheds (Table 1, Aitkenhead and McDowell 2000; Giesler et al. 2014; Jones and Schilling 2012; Khadka et al. 2014; Lopez et al. 2012; Wilson et al. 2013). In contrast, the Santa Fe River watershed annual area-normalized DIC export of 10.3 ton km^{-2} $year^{-1}$ is greater than that of many watersheds and did not vary greatly with flow regime [similar to that measured by Khadka et al. (2014)] (Table 1, Brunet et al. 2009; Giesler et al. 2014; Guo et al. 2012; Jones and Schilling 2012; Telmer and Veizer 1999).

The total dissolved C export rate for the Santa Fe River, 4.1×10^4 ton $year^{-1}$, represents a small fraction of the estimated 0.8–1.6 $\times$ 10^9 ton of dissolved C delivered by rivers to the global ocean each year (Ludwig et al. 1996; Suchet et al. 2003). However, assuming C exports from the Santa Fe River watershed are typical of karst watersheds, applying the annual area-normalized C export rate of 11.3 ton km^{-2} $year^{-1}$ to the 20 % of the Earth's ice-free land surface that is karst, yields the estimate that karst may be responsible for 18–36 % of the total C received by the ocean from rivers each year.

Summary and implications

A source water mixing model was used to evaluate watershed-scale C dynamic processes in this complex river-groundwater system. By taking into account the effects of mixing of several end member source waters, evidence was found for the occurrence and spatiotemporal heterogeneity of biogeochemical processes such as NDOM mineralization/production, carbonate dissolution/precipitation and NDOM sorption/desorption in the Santa Fe River watershed. These riparian zone processes were strongly mediated by watershed hydrogeology. For example, greater autotrophy occurred during average flow conditions and in the lower watershed, while greater NDOM mineralization was recorded during very low flow and in the upper watershed. In the upper watershed, carbonate dissolution was greater during low and very low flow, while carbonate precipitation was more common during average flow conditions. As a result of the combined effects of watershed hydrology and hydrogeology, the Santa Fe River watershed exports greater inorganic and organic C from the lower watershed than the upper watershed, and during average flow versus very low flow periods. Though spectrophotometric data showed NDOM in most samples to be mixtures of fresh and humified materials of both plant and microbial origin, NDOM exported from the lower watershed was generally more labile than that from the upper watershed.

The findings of this study have implications for riverine ecology. For example, subaquatic vegetation growth has been found to be closely linked with the riverine nutrient and oxygen dynamics (Heffernan et al. 2010; Schulz and Kohler 2006), both of which are tied to riparian zone C dynamics. Also, carbonate precipitation/dissolution likely influences concentrations of phosphorus (House 1990; Neal et al. 2002) and metals (Nimick et al. 2003; Zachara et al. 1991; Kurz et al. 2004) in these freshwater systems. In addition, the finding that, at least in this system, the subsurface produces labile NDOM in quantities that are comparable to or greater than that derived from soil flushing is one that has not been widely recognized by ecologists. Thus, changes in the hydrogeology of karst watersheds, either through groundwater withdrawals or climate change, can be expected to alter the biogeochemical cycling and ecology of their associated riverine-riparian systems and consequently the C fluxes from these watersheds. Given that karst watershed have been shown here to play in inordinately large role in terrestrial to marine C transfers and thus the global C cycle in general, they ought to receive greater study by geochemists.

Acknowledgments The authors thank Chad Foster for his help in the field, Jason Curtis for his assistance with the DIC and

C isotope measurements, and Kathleen McKee and Megan Wetherington for providing the hydrologic data. This work is supported by NSF Grant EAR-0853956.

References

Aitkenhead JA, McDowell WH (2000) Soil C : N ratio as a predictor of annual riverine DOC flux at local and global scales. Glob Biogeochem Cycles 14(1):127–138

Alberic P, Lepiller M (1998) Oxidation of organic matter in a karstic hydrologic unit supplied through stream sinks (Loiret, France). Water Res 32(7):2051–2064

Aravena R, Wassenaar LI, Spiker EC (2004) Chemical and carbon isotopic composition of dissolved organic carbon in a regional confined methanogenic aquifer. Isot Environ Health Stud 40(2):103–114

Batiot C, Emblanch C, Blavoux B (2003) Total Organic Carbon (TOC) and magnesium (Mg2 +): two complementary tracers of residence time in karstic systems. CR Geosci 335(2):205–214

Benner R, Opsahl S, ChinLeo G, Richey JE, Forsberg BR (1995) Bacterial carbon metabolism in the Amazon River system. Limnol Oceanogr 40(7):1262–1270

Berner RA (1999) A new look at the long-term carbon cycle. GSA Today 9:1–6

Berner RA, Lasaga AC (1989) Modeling the geochemical carbon-cycle. Sci Am 260(3):74–81

Brunet F et al (2009) Terrestrial and fluvial carbon fluxes in a tropical watershed: nyong basin Cameroon. Chem Geol 265(3–4):563–572

Burke EJ, Brown SJ, Christidis N (2006) Modeling the recent evolution of global drought and projections for the twenty-first century with the hadley centre climate model. J Hydrometeorol 7(5):1113–1125

Canfield DE Jr, Hoyer MV (1988) Influence of nutrient enrichment and light availability on the abundance of aquatic macrophytes in Florida streams. Can J Fish Aquat Sci 45(8):1467–1472

CCSP (2008) Reanalysis of historical climate data for key atmospheric features: implications for attribution of causes of observed change. A report by the U.S. Climate Change Science Program and the Subcommittee on Global Change Research, U.S. Environmental Protection Agency. Washington, DC. http://www.climatescience.gov/Library/sap/sap1-3/final-report/#finalreport.

Clark ID, Fritz P (1997) Environmental isotopes in hydrogeology. CRC press

Davis JA (1982) Adsorption of natural dissolved organic-matter at the oxide water interface. Geochim Cosmochim Acta 46(11):2381–2393

Dreybrodt W (1988) Processes in Karst Systems. Springer-Verlag, New York, p 288

Duarte CM et al (2010) Rapid accretion of dissolved organic carbon in the springs of Florida: the most organic-poor natural waters. Biogeosciences 7(12):4051–4057

Falkowski P et al (2000) The global carbon cycle: a test of our knowledge of earth as a system. Science 290(5490):291–296

Findlay SEG, Sinsabaugh RL (2003). Aquatic ecosystems: interactivity of dissolved organic matter Academic press

Ford DC, Williams PW (2007) Karst Hydrogeology and Geomorphology. Wiley, Chichester, p 562

Frimmel FH (1998) Characterization of natural organic matter as major constituents in aquatic systems. J Contam Hydrol 35(1–3):201–216

Frye GC, Thomas MM (1993) Adsorption of Organic-compounds on carbonate minerals. 2. Extraction of carboxylic-acids from recent and ancient carbonates. Chem Geol 109(1–4):215–226

Giesler R et al (2014) Catchment-scale dissolved carbon concentrations and export estimates across six subarctic streams in northern Sweden. Biogeosciences 11(2):525–537

Grubbs J.W (1998) Recharge rates to the upper Floridan aquifer in the Suwannee River Water Management District, Florida. U S geological survey water resources investigations Report 97-4283 30 p

Guo L, Cai Y, Belzile C, Macdonald RW (2012) Sources and export fluxes of inorganic and organic carbon and nutrient species from the seasonally ice-covered Yukon River. Biogeochemistry 107(1–3):187–206

Hancock PJ, Boulton AJ, Humphreys WF (2005) Aquifers and hyporheic zones: towards an ecological understanding of groundwater. Hydrogeol J 13(1):98–111

Heffernan JB et al (2010) Hydrologic and biotic influences on nitrate removal in a subtropical spring-fed river. Limnol Oceanogr 55(1):249–263

Hoch AR, Reddy MM, Aiken GR (2000) Calcite crystal growth inhibition by humic substances with emphasis on hydrophobic acids from the Florida Everglades. Geochim Cosmochim Acta 64(1):61–72

Houghton RA, Woodwell GM (1989) Global climatic-change. Sci Am 260(4):36–44

House WA (1990) The prediction of phosphate coprecipitation with calcite in fresh-waters. Water Res 24(8):1017–1023

Inskeep WP, Bloom PR (1986) Kinetics of calcite precipitation in the presence of water-soluble organic-ligands. Soil Sci Soc Am J 50(5):1167–1172

IPCC (2007) Climate change 2007: the physical basis. Contribution of working group I to the fourth assessment report of the intergovernmental panel on climate change. Cambridge University Press, Cambridge

Jin J (2012) Natural dissolved organic matter dynamics in a karstic surface-groundwater exchange system. Dissertation, University of Florida, Gainesville, FL, 168 pp

Jin J, Zimmerman AR (2010) Abiotic interactions of natural dissolved organic matter and carbonate aquifer rock. Appl Geochem 25(3):472–484

Jin J, Zimmerman AR, Moore PJ, Martin JB (2014) Organic and inorganic carbon dynamics of a karstic aquifer: Santa Fe River sink–rise system, north Florida, USA. J Geophys Res Biogeosci 119(3):340–357

Jones CS, Schilling KE (2012) Carbon export from the Raccoon River, Iowa: patterns, processes, and opportunities. J Environ Qual 42(1):155–163

Katz BG (1992) Hydrochemistry of the upper Floridan aquifer, Florida. US. Geological survey water-resources investigations report 91-4196, 37, p 10

Khadka MB, Martin JB, Jin J (2014) Transport of dissolved carbon and CO_2 degassing from a river system in a mixed silicate and carbonate catchment. J Hydrol 513:391–402

Kortelainen NM, Karhu JA (2006) Tracing the decomposition of dissolved organic carbon in artificial groundwater recharge using carbon isotope ratios. Appl Geochem 21(4):547–562

Kurz RC et al (2004) Mapping and monitoring submerged aquatic vegetation in Ichetucknee springs. Suwanee River Water Management District, Live Oak

Laurion I, Vincent WF, Lean DRS (1997) Underwater ultraviolet radiation: development of spectral models for northern high latitude lakes. Photochem Photobiol 65(1):107–114

Lee ES, Krothe NC (2001) A four-component mixing model for water in a karst terrain in south-central Indiana, USA. Using solute concentration and stable isotopes as tracers. Chem Geol 179(1–4):129–143

Lee JU, Lee SW, Kim KW, Yoon CH (2005) The effects of different carbon sources on microbial mediation of arsenic in arsenic-contaminated sediment. Environ Geochem Health 27(2):159–168

Li S-L et al (2010) Geochemistry of dissolved inorganic carbon and carbonate weathering in a small typical karstic catchment of Southwest China: isotopic and chemical constraints. Chem Geol 277(3–4):301–309

Lin YP, Singer PC (2005) Inhibition of calcite crystal growth by polyphosphates. Water Res 39(19):4835–4843

Lindroos AJ, Kitunen V, Derome J, Helmisaari HS (2002) Changes in dissolved organic carbon during artificial recharge of groundwater in a forested esker in Southern Finland. Water Res 36(20):4951–4958

Liu Z, Zhao J (2000) Contribution of carbonate rock weathering to the atmospheric CO2 sink. Environ Geol 39(9):1053–1058

Liu Z, Dreybrodt W, Liu H (2011) Atmospheric CO2 sink: silicate weathering or carbonate weathering? Appl Geochem 26:S292–S294

Lopez R, Del Castillo CE, Miller RL, Salisbury J, Wisser D (2012) Examining organic carbon transport by the Orinoco River using SeaWiFS imagery. J Geophys Res Biogeosci 117(17):9721–9742

Lovley DR, Chapelle FH (1995) Deep subsurface microbial processes. Rev Geophys 33(3):365–381

Lovley DR, Chapelle FH (1996) Hydrogen-based microbial ecosystems in the Earth. Science 272(5263): 896–896

Ludwig W, AmiotteSuchet P, Probst JL (1996) River discharges of carbon to the world's oceans: determining local inputs of alkalinity and of dissolved and particulate organic carbon. Comptes Rendus De L Academie Des Sciences Serie Ii Fascicule a-Sciences De La Terre Et Des Planetes 323(12):1007–1014

Martin JB, Dean RW (2001) Exchange of water between conduits and matrix in the Floridan aquifer. Chemical Geology 179:145–165

Martin JB, Gordon SL (2000) Surface and ground water mixing, flow paths, and temporal variations in chemical compositions and karst springs. In: Sasowsky ID, Wicks CM (eds) Groundwater flow and contaminant transport in carbonate aquifers. A. A Balkema, Amsterdam, pp 65–92

Martin JB, Brown A, Ezell J (2013) Do carbonate karst terrains affect the global carbon cycle? Acta Carsologica 42(2–3): 187–196

McCarthy JF et al (1996) Field tracer tests on the mobility of natural organic matter in a sandy aquifer. Water Resour Res 32(5):1223–1238

McKnight DM et al (2001) Spectrofluorometric characterization of dissolved organic matter for indication of precursor organic material and aromaticity. Limnol Oceanogr 46(1):38–48

McMahon PB (2001) Aquifer/aquitard interfaces: mixing zones that enhance biogeochemical reactions. Hydrogeol J 9(1):34–43

Meyer JL, Edwards RT, Risley R (1987) Bacterial-growth on dissolved organic carbon from a blackwater river. Microb Ecol 13(1):13–29

Moore PJ, Martin JB, Screaton EJ (2009) Geochemical and statistical evidence of recharge, mixing, and controls on spring discharge in an eogenetic karst aquifer. J Hydrol 376(3–4):443–455

Moran MA, Sheldon WM, Sheldon JE (1999) Biodegradation of riverine dissolved organic carbon in five estuaries of the southeastern United States. Estuaries 22(1):55–64

Morris DP et al (1995) The attentuation of solar UV radiation in lakes and the role of dissolved organic carbon. Limnol Oceanogr 40(8):1381–1391

Neal C et al (2002) Phosphorus-calcium carbonate saturation relationships in a lowland chalk river impacted by sewage inputs and phosphorus remediation: an assessment of phosphorus self-cleansing mechanisms in natural waters. Sci Total Environ 282:295–310

Nimick DA et al (2003) Diel cycles in dissolved metal concentrations in streams: occurrence and possible causes. Water Resour Res 39(9):1247–1264

Ohno T (2002) Fluorescence inner-filtering correction for determining the humification index of dissolved organic matter. Environ Sci Technol 36(4):742–746

Pabich WJ, Valiela I, Hemond HF (2001) Relationship between DOC concentration and vadose zone thickness and depth below water table in groundwater of Cape Cod USA. Biogeochemistry 55(3):247–268

Pearlstine LG (2009) Potential Ecological consequences of climate change in South Florida and the Everglades: 2008 literature Synthesis South Florida Natural Resources Center, Everglades National Park. Homstead, FL

Petrone KC, Fellman JB, Hood E, Donn MJ, Grierson PF (2011) The origin and function of dissolved organic matter in agro-urban coastal streams. J Geophys Res-Biogeosci 116:13

Petrovic M, Kastelan-Macan M, Horvat AJM (1999) Interactive sorption of metal ions and humic acids onto mineral particles. Water Air Soil Pollut 111(1–4):41–56

Probst JL, Mortatti J, Tardy Y (1994) Carbon river fluxes and weathering CO2 consumption in the Congo and Amazon River basins. Appl Geochem 9(1):1–13

Pronk M, Goldscheider N, Zopfi J (2006) Dynamics and interaction of organic carbon, turbidity and bacteria in a karst aquifer system. Hydrogeol J 14(4):473–484

Quay P (1992) Carbon sink: the role of oceans. Geotimes 37(9):16–18

Randazzo AF, Jones DS (1997). The geology of Florida. University Press of Florida

Rauch T, Drewes L (2004) Assessing the removal potential of soil-aquifer treatment systems for bulk organic matter. Water Sci Technol 50(2):245–253

Saunders TJ, Collins ME, Frazer TK Hurt G.W (2007). The distribution and function of biogeochemical interfaces,

gradients, and fluxes in a coastal spring-fed riverine and estuarine system. Ecological society of America annual meeting abstracts

Schulz M, Kohler J (2006) A simple model of phosphorus retention evoked by submerged macrophytes in lowland rivers. Hydrobiologia 563:521–525

Scott TM (1988) The lithostratigraphy of the Hawthorn Group (Miocene) of Florida USA. Florida Dep Nat Resour Bureau Geol Bull 59:XII–148

Screaton E, Martin JB, Ginn B, Smith L (2004) Conduit properties and karstification in the unconfined Floridan Aquifer. Ground Water 42(3):338–346

Selman C, Misra V, Stefanova L, Dinapoli S, Smith TJ III (2013) On the twenty-first-century wet season projections over the Southeastern United States. Reg Environ Change 13:S153–S164

Suchet PA, Probst JL, Ludwig W (2003). Worldwide distribution of continental rock lithology: Implications for the atmospheric/soil CO2 uptake by continental weathering and alkalinity river transport to the oceans. Global Biogeochem Cycles 17(2) 1038

Telmer K, Veizer J (1999) Carbon fluxes, pCO(2) and substrate weathering in a large northern river basin, Canada: carbon isotope perspectives. Chem Geol 159(1–4):61–86

Thomas MM, Clouse JA, Longo JM (1993) Adsorption of organic-compounds on carbonate minerals. 3. influence on dissolution rates. Cheml Geol 109(1–4):227–237

Upchurch SB, Lawrence FW (1984) Impact of ground water chemistry on sinkhole development along a retreating scarp. In: Beck BF (ed) Sinkholes: their geology, engineering, and environmental impact. A.A. Balkema, Rotterdam, pp 189–195

Watson RT, Rodhe H, Oeschger H, Siegenthaler U (1990). Greenhouse gases and aerosols. In: JT Houghton, GJ Jenkins EJJ (Eds), Climate change: the IPCC scientific assessment. Cambridge University Press, Cambridge, pp. 1–40.

Wetzel RG (2001) Limnology: lake and river ecosystems. Academic Press, San Diego

White WB (1988) Geomorphology and hydrology of Karst Terrains. Oxford University Press, New York, p 464

Wilson HF, Saiers JE, Raymond PA, Sobczak WV (2013) Hydrologic drivers and seasonality of dissolved organic carbon concentration, nitrogen content, bioavailability, and export in a forested new england stream. Ecosystems 16(4):604–616

Zachara JM, Cowan CE, Resch CT (1991) Sorption of divalent metals on calcite. Geochim Cosmochim Acta 55(6):1549–1562

Zsolnay A, Baigar E, Jimenez M, Steinweg B, Saccomandi F (1999) Differentiating with fluorescence spectroscopy the sources of dissolved organic matter in soils subjected to drying. Chemosphere 38(1):45–50